Nonlinear Optics of THz (and IR and FIR) Radiation

Robert W. Boyd

Department of Physics and
School of Electrical Engineering and Computer Science
University of Ottawa

The Institute of Optics and
Department of Physics and Astronomy
University of Rochester

With many collaborators, especially Ksenia Dolgaleva and Jean-Michel Ménard.

The visuals of this talk will be posted at boydnlo.ca/presentations

Presented at the 48th Conference on Infrared, Millimeter. and Terahertz Waves,
Montréal QC, Canada, September 18, 2023.

Nonlinear Optics of Infrared Radiation

- The early experiments of nonlinear optics were all performed using a ruby laser operating at 6943 angstroms.
- By certain definitions, 6943 angstroms is an infrared wavelength.
- But for the purposes of this talk, I will exclude ruby laser experiments from the discussion of nonlinear optics of IR radiation

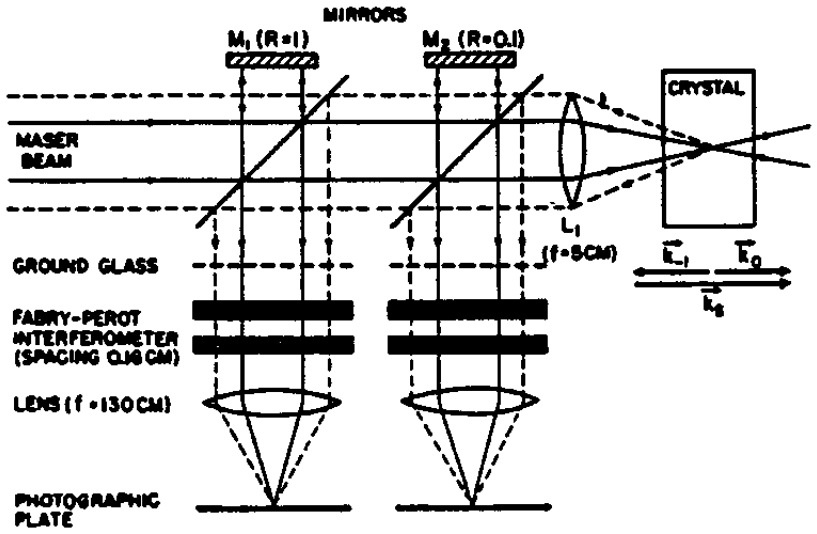

Stimulated Brillouin Scattering, Chiao, Townes, and Stoicheff (1964)

Imaging Upconversion

"Noise-free" conversion of infrared images to the visible.
Proposed by Midwinter and Warner (1967).

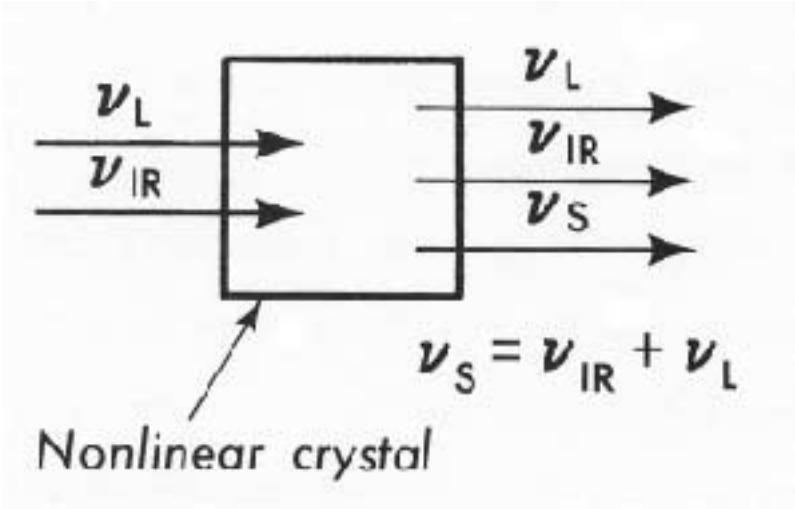

Phase-matching requirements ensure that image information is preserved.

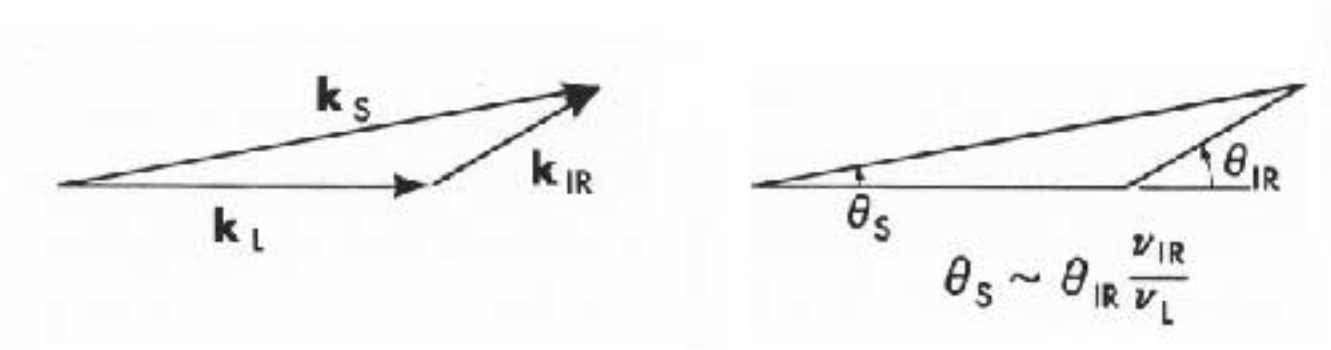

Astronomical Imaging Upconversion

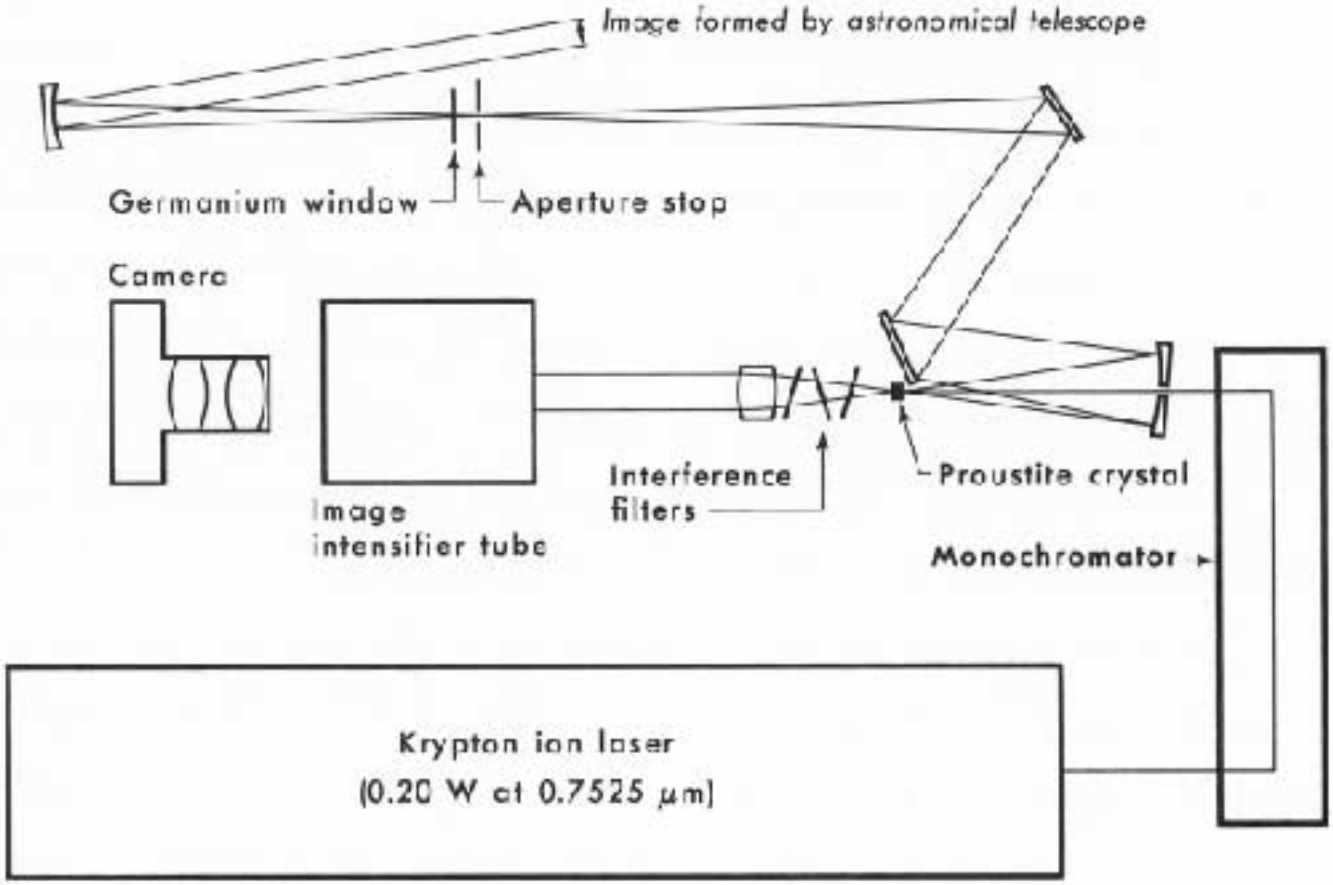

laboratory sources

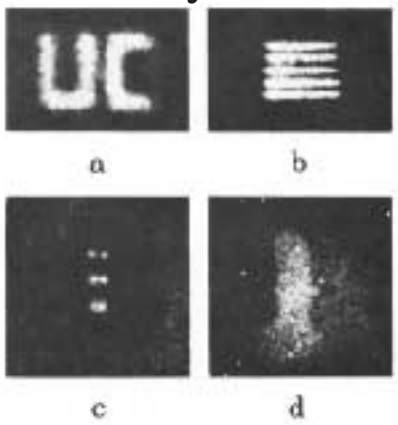

astronomical sources

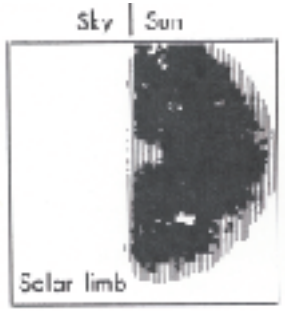

R. W. Boyd and C. H. Townes Appl. Phys. Lett. 33 440 (1977).

Resolution of Astronomical Telescopes

- Wavelength dependence under turbulence-dominated conditions
- Images are sharper in the infrared than in the visible!

  (D. L. Fried, R. E. Hufnagel, V. I. Tatarski)
- IR data obtained using infrared upconversion

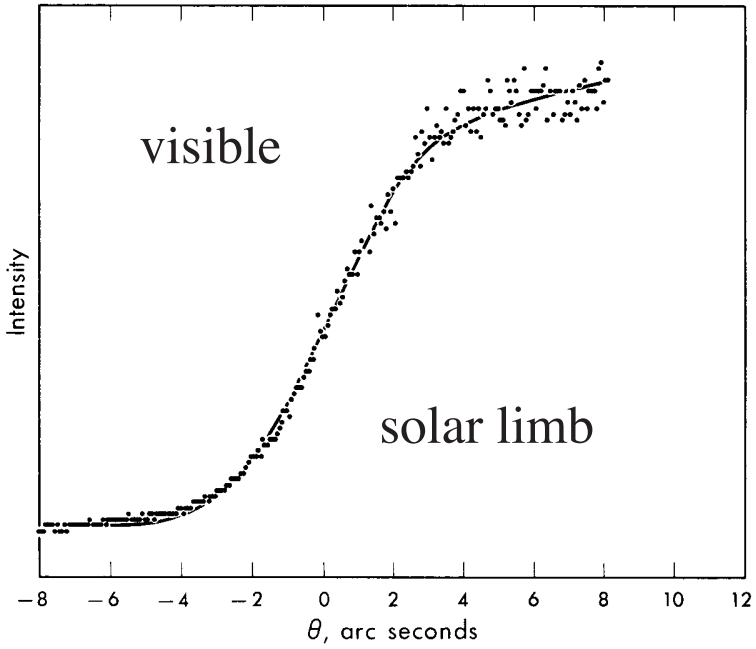

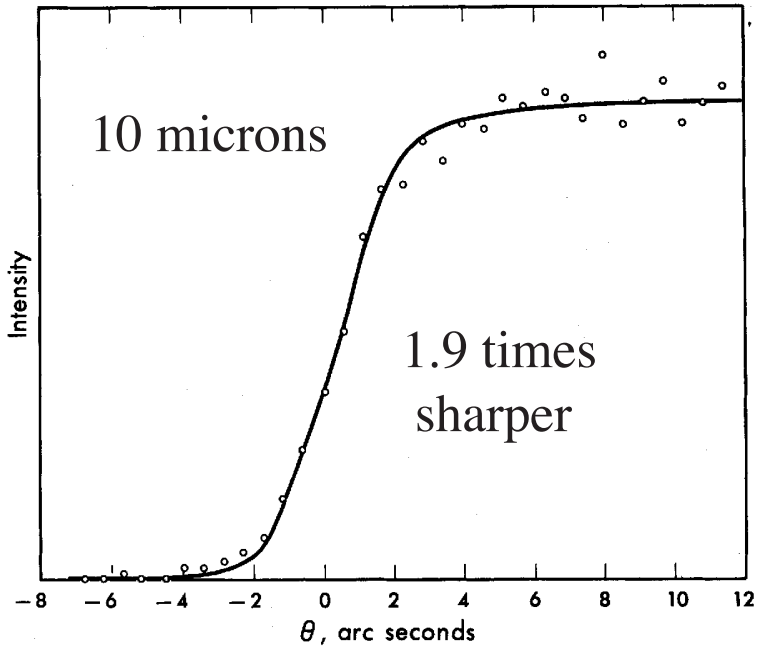

R. W. Boyd, J. Opt. Soc. Am. 68, 877, 1978.

Upconversion of Single Photons with 99% Efficiency

- Uses pulsed pump laser (high peak power)
- Uses periodically poled lithium niobate (highly nonlinear)
- Detects single-transverse mode field (no image information)

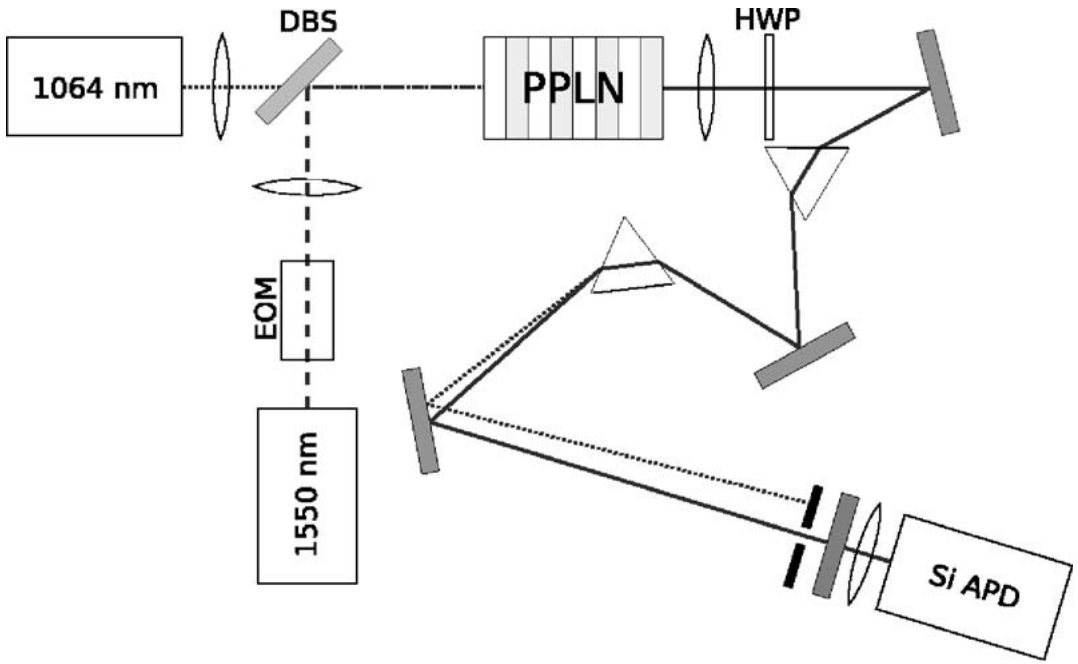

Extremely promising for quantum information studies. (Preserves coherence.)

VanDevender and Kwiat, J. Opt. Soc. Am. B 24, 295 (2007).

Nonlinear Optical Methods to Generate THz Radiation

- Difference-frequency generation

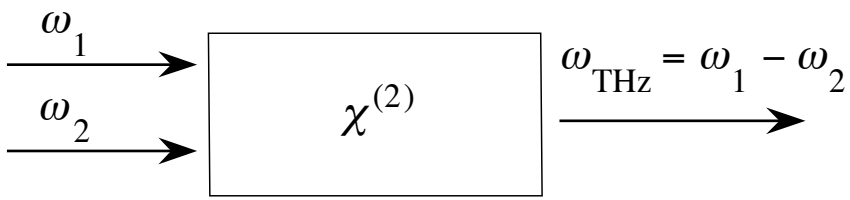

- Optical rectification

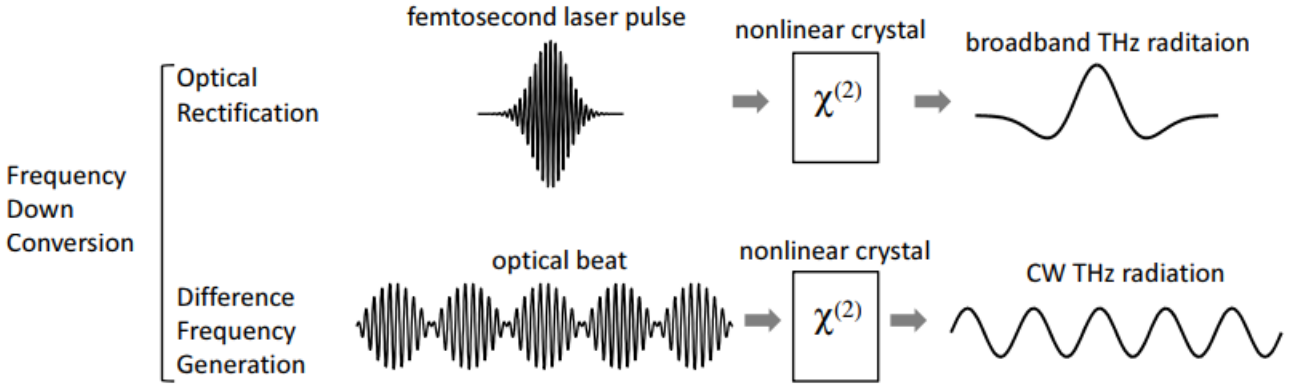

- Hebling's tilted pulse-front method

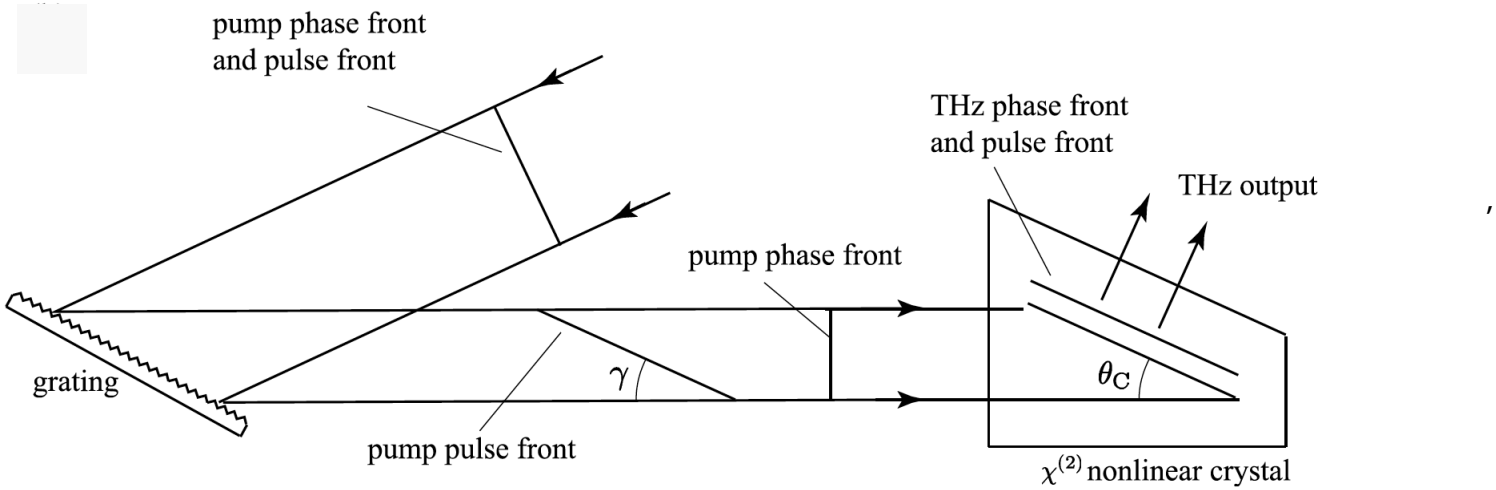

Huge Phonon-Mediated THz Nonlinear Response

Recent theoretical and laboratory work has shown that third-order nonlinear response ($\chi^{(3)}$ and n_2) are orders of magnitude larger than values for the same material at visible frequencies.

Theoretical models that accurately describe these results ascribe the origin of this huge response to vibrational (phonon) resonances.

n_2

In collaboration with

Prof. Sergei Kozlov **Daria Materikina**

State University of Information Technologies, Mechanics and Optics, Saint Petersburg, Russia

K. Dolgaleva, D. Materikina, R. W. Boyd, and S. A. Kozlov, "Prediction of Extremely Large Nonlinear Refractive Index for Crystals at Terahertz Frequencies," Phys. Rev. A **92**, 023809 (2015).

uOttawa

Prediction of extremely large value of n_2

Polarization $\quad P = \chi_{\text{eff}} E$

Susceptibility $\quad \chi_{\text{eff}} = \chi^{(1)} + 3\chi^{(3)}|E|^2$

Refractive index $\quad \tilde{n} = \sqrt{1 + 4\pi\chi_{\text{eff}}} = \tilde{n}_0 + \tilde{n}_2 I$

Kerr coefficient or nonlinear refractive index

(We use Gaussian units but convert to SI at the end.)

Electronic and Vibrational Response

$$P = P_{\mathrm{el}} + P_{\mathrm{v}} = \chi_{\mathrm{eff}} E$$

electronic vibrational

$$\chi_{\mathrm{eff}} = \chi^{(1)} + 3\chi^{(3)}|E|^2$$

$$\chi^{(1)} = \chi^{(1)}_{\mathrm{el}} + \chi^{(1)}_{\mathrm{v}} \qquad \chi^{(3)} = \chi^{(3)}_{\mathrm{el}} + \chi^{(3)}_{\mathrm{v}}$$

Dominant at THz frequencies

Our Model

We analyze the vibrational nonlinearity of a crystal by considering the dynamics of ions in the lattice

1. Starting from the classical anharmonic oscillator:

$$\ddot{x} + 2\gamma\dot{x} + \omega_0^2 x + ax^2 + bx^3 = \alpha E$$

deviation of an ion — damping coefficient — nonlinear coefficients

$$\alpha = \frac{q}{m}$$

2. Perturbation theory:

$$\ddot{x} + 2\gamma\dot{x} + \omega_0^2 x + ax^2 + bx^3 = \lambda\alpha E$$

$$0 \leq \lambda \leq 1$$

Look for a solution in the form

$$x = \lambda x^{(1)} + \lambda^2 x^{(2)} + \lambda^3 x^{(3)} + \ldots$$

uOttawa

Our Model

3. Split into three equations:

$$\ddot{x}^{(1)} + 2\gamma\dot{x}^{(1)} + \omega_0^2 x^{(1)} = \alpha E,$$

$$\ddot{x}^{(2)} + 2\gamma\dot{x}^{(2)} + \omega_0^2 x^{(2)} + a[x^{(1)}]^2 = 0,$$

$$\ddot{x}^{(3)} + 2\gamma\dot{x}^{(3)} + \omega_0^2 x^{(3)} + 2a x^{(1)} x^{(2)} + b[x^{(1)}]^3 = 0.$$

Consider the oscillations of the ions at the fundamental frequency:

$$E(\omega) = E_\omega \mathrm{e}^{-i\omega t} + \mathrm{c.\,c.} \qquad x = x_\omega \mathrm{e}^{-i\omega t} + \mathrm{c.\,c.}$$

Our Model

4. Final expression for x_ω :

$$x_\omega = \frac{\alpha E_\omega}{\omega_0^2 - \omega^2 - 2\gamma i\omega} + \frac{1}{(\omega_0^2 - \omega^2 - 2\gamma i\omega)^4} \times \left[2a^2\alpha^3 \frac{3\omega_0^2 - 8\omega^2 - 8\gamma i\omega}{\omega_0^2(\omega_0^2 - 4\omega^2 - 4\gamma i\omega)} + 3b\alpha^3 \right] |E_\omega|^2 E_\omega$$

Our Model

5. Relating the deviation to the polarization:

$$P = P_{\mathrm{el}} + P_{\mathrm{v}} = Nqx = P_{\omega}\mathrm{e}^{-i\omega t} + \mathrm{c.c.}$$

electronic vibrational

$$P_{\omega} = \chi^{(1)}E_{\omega} + 3\chi^{(3)}|E_{\omega}|^2 E_{\omega} \qquad P_{\omega} = \chi_{\mathrm{eff}}E_{\omega}$$

Effective susceptibility:

$$\chi_{\mathrm{eff}} = \chi^{(1)} + 3\chi^{(3)}|E_{\omega}|^2$$
$$= \chi^{(1)}_{\mathrm{el}} + \chi^{(1)}_{\mathrm{v}} + 3\chi^{(3)}_{\mathrm{el}}|E_{\omega}|^2 + 3\chi^{(3)}_{\mathrm{v}}|E_{\omega}|^2$$

Our Model

6. Expressing the susceptibilities:

$$\chi^{(1)} = qN \frac{\alpha}{\omega_0^2 - \omega^2 - 2\gamma i\omega}$$

$$\chi^{(3)} = \frac{qN}{3} \frac{\alpha^3}{(\omega_0^2 - \omega^2 - 2\gamma i\omega)^4} \times \left[2a^2 \frac{3\omega_0^2 - 8\omega^2 - 8\gamma i\omega}{\omega_0^2(\omega_0^2 - 4\omega^2 - 4\gamma i\omega)} + 3b \right]$$

Our Model

7. Expressing the complex overall refractive index:

$$\tilde{n}^2 = 1 + 4\pi\chi_{\text{eff}} \qquad \tilde{n} = \tilde{n}_0 + 2\tilde{\bar{n}}_2|E_\omega|^2$$

$$\tilde{n}_0^2 + 4\tilde{n}_0\tilde{\bar{n}}_2|E_\omega|^2 = 1 + 4\pi\chi^{(1)} + 12\pi\chi^{(3)}|E_\omega|^2$$

Expressing the linear and nonlinear <u>complex</u> refractive indices:

$$\tilde{n}_0 = \sqrt{1 + 4\pi\chi^{(1)}}$$

$$\tilde{\bar{n}}_2 = \tilde{\bar{n}}_{2,\,\text{el}} + \tilde{\bar{n}}_{2,\,\text{v}} = \frac{3\pi\chi^{(3)}}{\tilde{n}_0}$$

electronic vibrational

uOttawa

Our Model

8. Final expression for the Kerr coefficient:

$$\bar{\tilde{n}}_2 = \frac{\pi q N}{\tilde{n}_0} \frac{\alpha^3}{(\omega_0^2 - \omega^2 - 2\gamma i\omega)^4} \times \left[2a^2 \frac{3\omega_0^2 - 8\omega^2 - 8\gamma i\omega}{\omega_0^2(\omega_0^2 - 4\omega^2 - 4\gamma i\omega)} + 3b \right]$$

Our Model

9. Nonlinear refractive index and absorption

$$\bar{n}_2 = \mathrm{Re}\,(\tilde{\bar{n}}_2) = 3\pi\,\mathrm{Re}\left(\frac{\chi^{(3)}}{\sqrt{1+4\pi\chi^{(1)}}}\right)$$

$$\alpha_2 = \frac{2\omega}{c}\,\mathrm{Im}\,(\tilde{\bar{n}}_2) = 6\pi\frac{\omega}{c}\,\mathrm{Im}\left(\frac{\chi^{(3)}}{\sqrt{1+4\pi\chi^{(1)}}}\right)$$

Our Model

10. In the low-frequency limit:

$$\bar{n}_{2,\mathrm{v}}^{\omega \ll \omega_0} \approx \frac{\pi q N}{n_0}\left(\frac{6a^2\alpha^3}{\omega_0^{10}} + \frac{3b\alpha^3}{\omega_0^{8}}\right)$$

$$\bar{n}_{2,\mathrm{v}}^{\omega \ll \omega_0} = \bar{n}_{2,\mathrm{v}}^{(1)} + \bar{n}_{2,\mathrm{v}}^{(2)}$$

Thermal expansion Dynamic Stark effect

We next estimate the two contributions using the parameters of crystal quartz

Crystal Quartz Parameters

$\alpha_T = 7.6 \times 10^{-6}\ (^oC)^{-1}$ - thermal expansion coefficient

$\omega_0 = 2.34 \times 10^{14}$ rad - vibrational resonance frequency

$m = 1.69 \times 10^{-23}$ g - reduced mass of vibrational mode

$N = 2.65 \times 10^{22}\ cm^{-3}$ - molecular density

$a_l = 5.24\ \mathring{A}$ - lattice constant

Linear refractive index

$$n_0^{(\omega \ll \omega_0)} = \sqrt{1 + 4\pi\chi_{el}^{(1),\,\omega \ll \omega_0} + 4\pi\chi_v^{(1),\,\omega \ll \omega_0}} = 2.1$$

$$n_{0,\,el}^{(\omega \ll \omega_0)} = 1.4 \longrightarrow n_{0,\,v}^{(\omega \ll \omega_0)} = 1.8$$

Numerical Example

First – in terms of thermal expansion coefficient

$$\bar{n}^{(1)}_{2,\,\mathrm{v}} = \frac{\pi q N}{n_0}\,\frac{6a^2\alpha^3}{\omega_0^{10}}$$

$$\alpha_{\mathrm{T}} = -\frac{a k_{\mathrm{B}}}{m\omega_0^4 a_{\mathrm{l}}}$$

$$\alpha = \frac{\omega_0^2}{4\pi q N}\left[(n_{0,\,\mathrm{v}}^{\omega\ll\omega_0})^2 - 1\right]$$

Numerical Example

Estimated values of n_2 :

The two contributions:

$$\bar{n}_{2,\,\mathrm{v}}^{(1)} \approx 2.24 \times 10^{-9}\ \mathrm{esu}$$

$$\bar{n}_{2,\,\mathrm{v}}^{(2)} \approx -3.27 \times 10^{-11}\ \mathrm{esu}$$

In esu:

$$\bar{n}_{2,\,\mathrm{v}} \approx 2.21 \times 10^{-9}\ \mathrm{esu}$$

In m²/W:

$$n_{2,\,\mathrm{v}}^{(\omega \ll \omega_0)} = 4.42 \times 10^{-16}\ \mathrm{m^2/W}$$

Compare to the value in visible:

$$n_2 = 3 \times 10^{-20}\ \mathrm{m^2/W}$$

Dispersion Curves

Strong resonance at 37.2 THz.
Weaker resonances at 7.9 and 3.9 THz.

$$\bar{\tilde{n}}_2 = \frac{\pi q N}{\tilde{n}_0} \frac{\alpha^3}{(\omega_0^2 - \omega^2 - 2\gamma i\omega)^4} \times \left[2a^2 \frac{3\omega_0^2 - 8\omega^2 - 8\gamma i\omega}{\omega_0^2(\omega_0^2 - 4\omega^2 - 4\gamma i\omega)} + 3b \right]$$

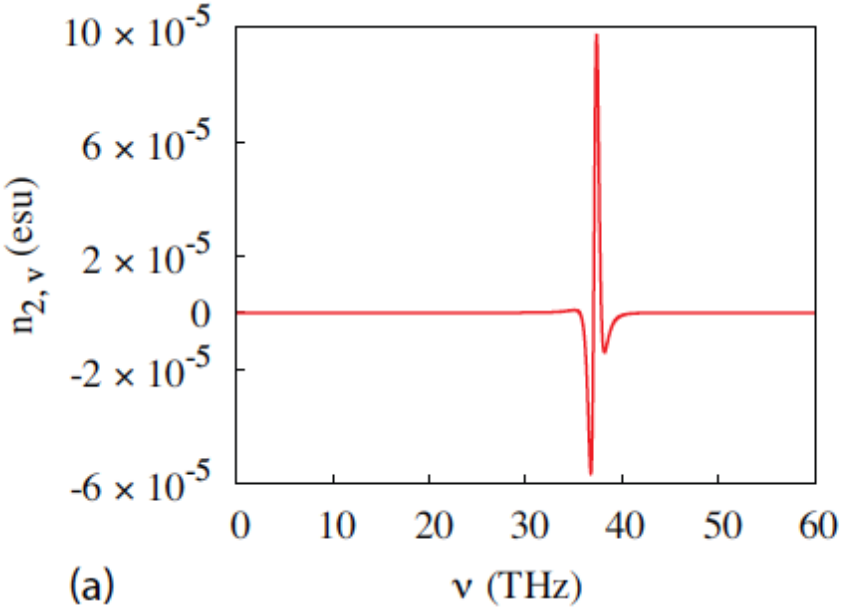

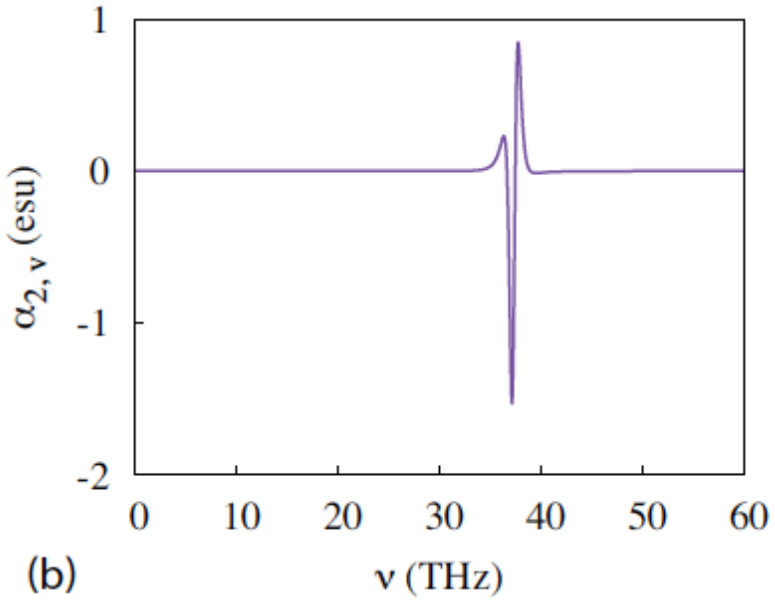

uOttawa

Dispersion Curves

A two-photon resonance occurs at 37.2 THz/2 = 18.6 THz

$$\tilde{\bar{n}}_2 = \frac{\pi q N}{\tilde{n}_0} \frac{\alpha^3}{(\omega_0^2 - \omega^2 - 2\gamma i\omega)^4} \times \left[2a^2 \frac{3\omega_0^2 - 8\omega^2 - 8\gamma i\omega}{\omega_0^2(\omega_0^2 - 4\omega^2 - 4\gamma i\omega)} + 3b \right]$$

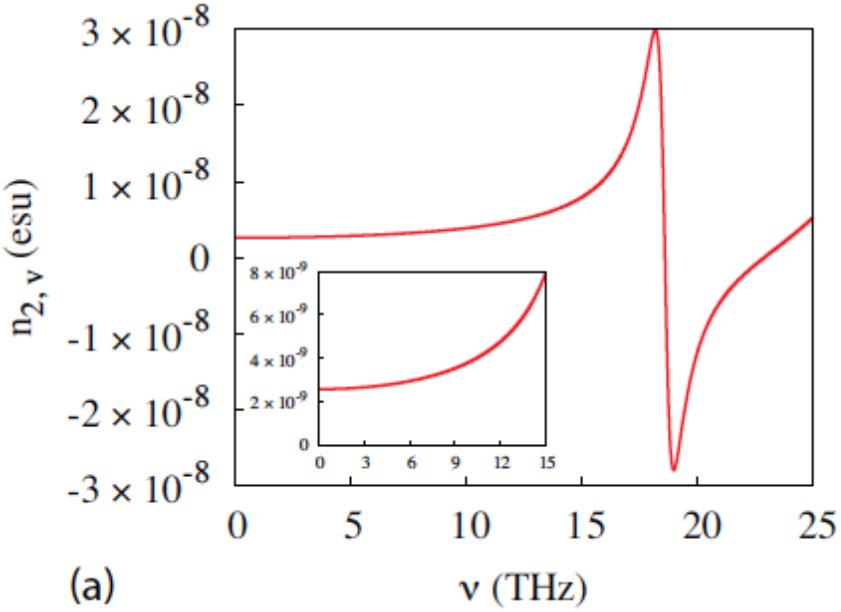

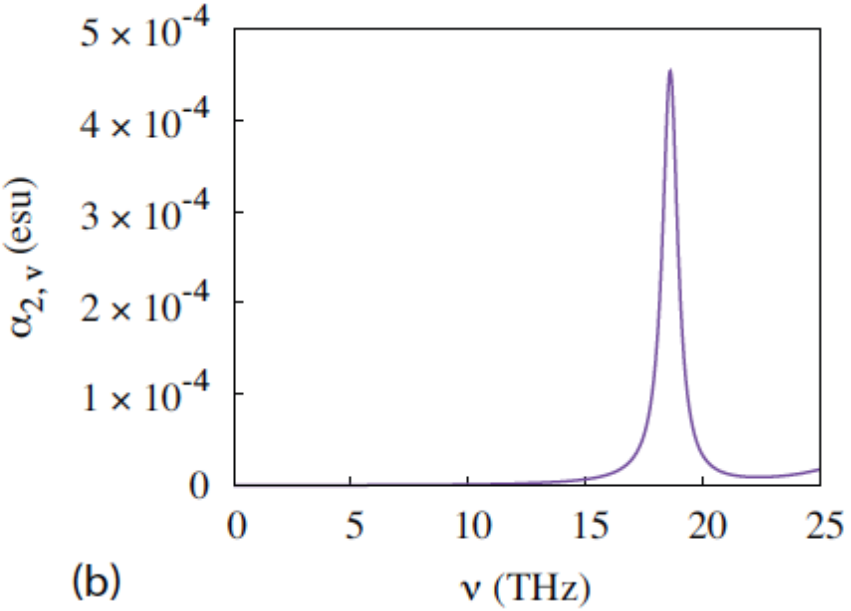

uOttawa

In Summary:

- Simple model is proposed

$$\bar{\tilde{n}}_2 = \frac{\pi q N}{\tilde{n}_0} \frac{\alpha^3}{(\omega_0^2 - \omega^2 - 2\gamma i\omega)^4} \times \left[2a^2 \frac{3\omega_0^2 - 8\omega^2 - 8\gamma i\omega}{\omega_0^2(\omega_0^2 - 4\omega^2 - 4\gamma i\omega)} + 3b \right]$$

- Estimated value of vibrational n_2 in THz range is very large

$$n_{2,\,\mathrm{v}}^{(\omega \ll \omega_0)} = 4.42 \times 10^{-16}\ \mathrm{m}^2/\mathrm{W}$$

- Interesting resonant behaviour is revealed

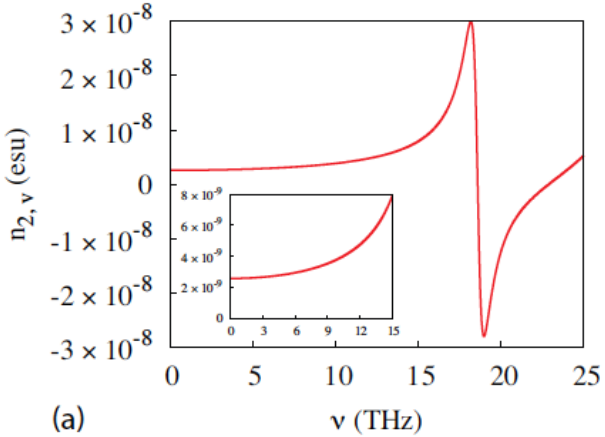

uOttawa

Measurement of Nonlinear OpticalResponse of Quartz

RESEARCH ARTICLE

ADVANCED OPTICAL MATERIALS
www.advopticalmat.de

Strong Nonlinear Response in Crystalline Quartz at THz Frequencies

*Soheil Zibod, Payman Rasekh, Murat Yildrim, Wei Cui, Ravi Bhardwaj, Jean-Michel Ménard, Robert W. Boyd, and Ksenia Dolgaleva**

Adv. Optical Mater. 2023, 2202343

Previous works

$10^2 \times n_2^{opt}$

Terahertz Kerr effect

Matthias C. Hoffmann,[1,2,a)] Nathaniel C. Brandt,[2] Harold Y. Hwang,[2] Ka-Lo Yeh,[2] and Keith A. Nelson[2]

$10^6 \times n_2^{opt}$

Giant Third-Order Nonlinear Response of Liquids at Terahertz Frequencies

Anton Tcypkin,[1,*] Maria Zhukova,[1] Maksim Melnik,[1] Irina Vorontsova,[1] Maksim Kulya,[1] Sergey Putilin,[1] Sergei Kozlov,[1] Saumya Choudhary,[2] and Robert W. Boyd[2,3]

$10^2 \times n_2^{opt}$

Terahertz-induced Kerr effect in amorphous chalcogenide glasses

M. Zalkovskij,[1,a)] A. C. Strikwerda,[1] K. Iwaszczuk,[1] A. Popescu,[2] D. Savastru,[2] R. Malureanu,[1] A. V. Lavrinenko,[1] and P. U. Jepsen[1]

$10^{24} \times n_2^{opt}$

Terahertz Nonlinear Spectroscopy of Water Vapor

Payman Rasekh,* Akbar Safari,* Murat Yildirim, Ravi Bhardwaj, Jean-Michel Ménard, Ksenia Dolgaleva, and Robert W. Boyd

$10^3 \times n_2^{opt}$

Terahertz Kerr effect in gallium phosphide crystal

M. Cornet,[1,2] J. Degert,[1,2,*] E. Abraham,[1,2] and E. Freysz[1,2]

Prediction of an extremely large nonlinear refractive index for crystals at terahertz frequencies

Ksenia Dolgaleva,[1,*] Daria V. Materikina,[2] Robert W. Boyd,[1] and Sergei A. Kozlov[2]

$10^4 \times n_2^{opt}$

Detection: Electro-Optic Sampling

Pockels effect

$$P_i = 2\sum_{j,k} \epsilon_0 \chi^{(2)}_{i,j,k}(\omega, \omega, 0) E_j(\omega) E_k(0)$$

Phase retardation $\Delta\phi = \frac{\omega L}{c} n_0^3 r_{41} E_{\mathrm{THz}}$

$$I_x = \frac{I_0}{2}(1 - \Delta\Phi)$$

$$I_y = \frac{I_0}{2}(1 + \Delta\Phi) \qquad I_s = I_y - I_x \propto E_{THz}$$

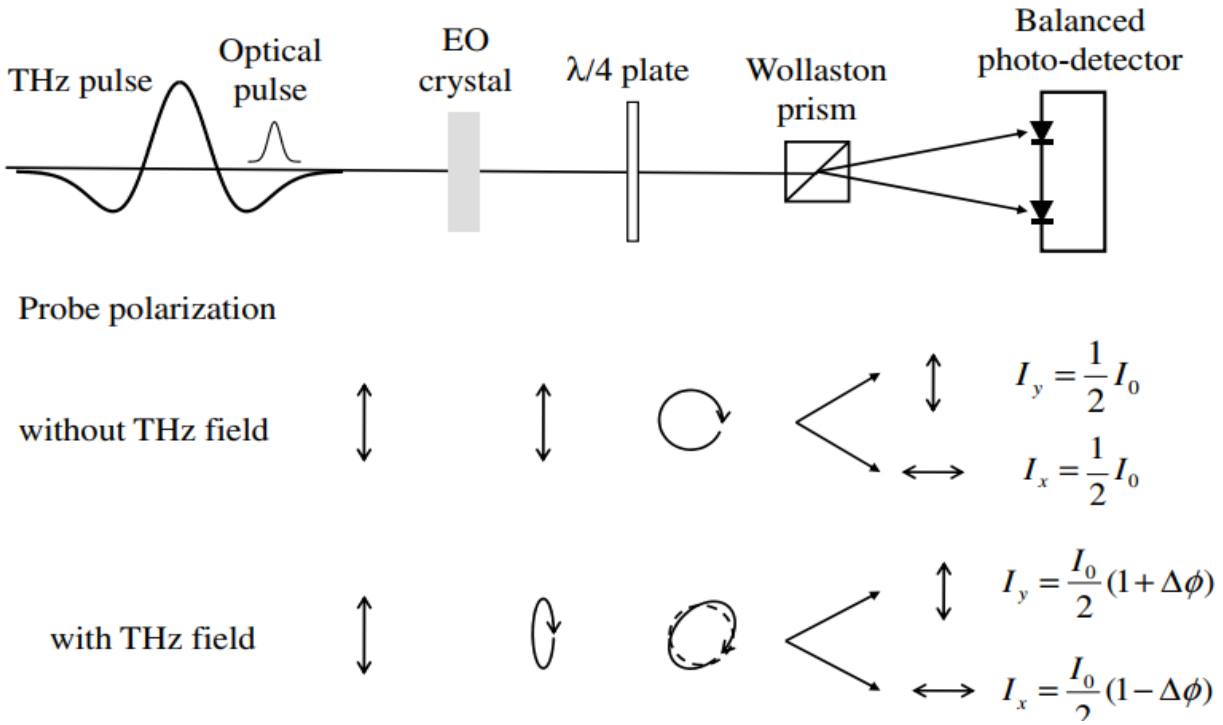

THz detection with EO sampling [1]

THz Time Domain Spectroscopy (THz-TDS)

- Time domain
- Single-cycle pulse
- E/O sampling → magnitude and phase
- Absorption coefficient and refractive index

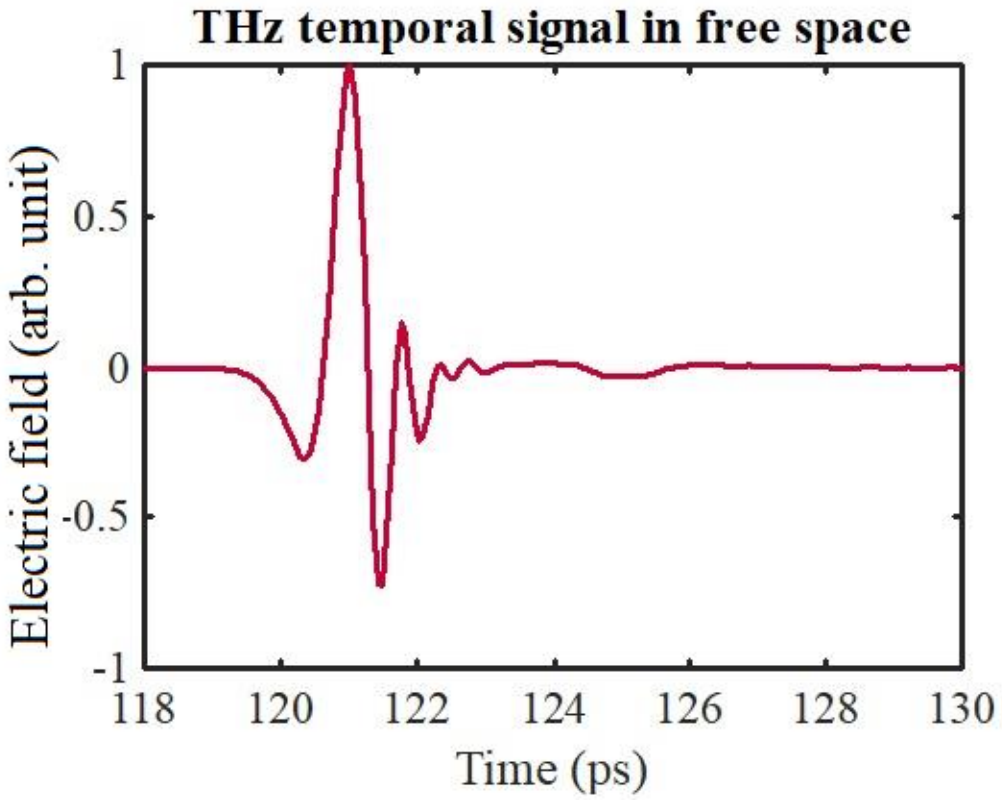

Experimental Setup

- Optical Rectification in $LiNbO_3$
- Pulse front tilting
- E/O sampling
- 225 kV/cm at focus
- 1mm crystalline quartz

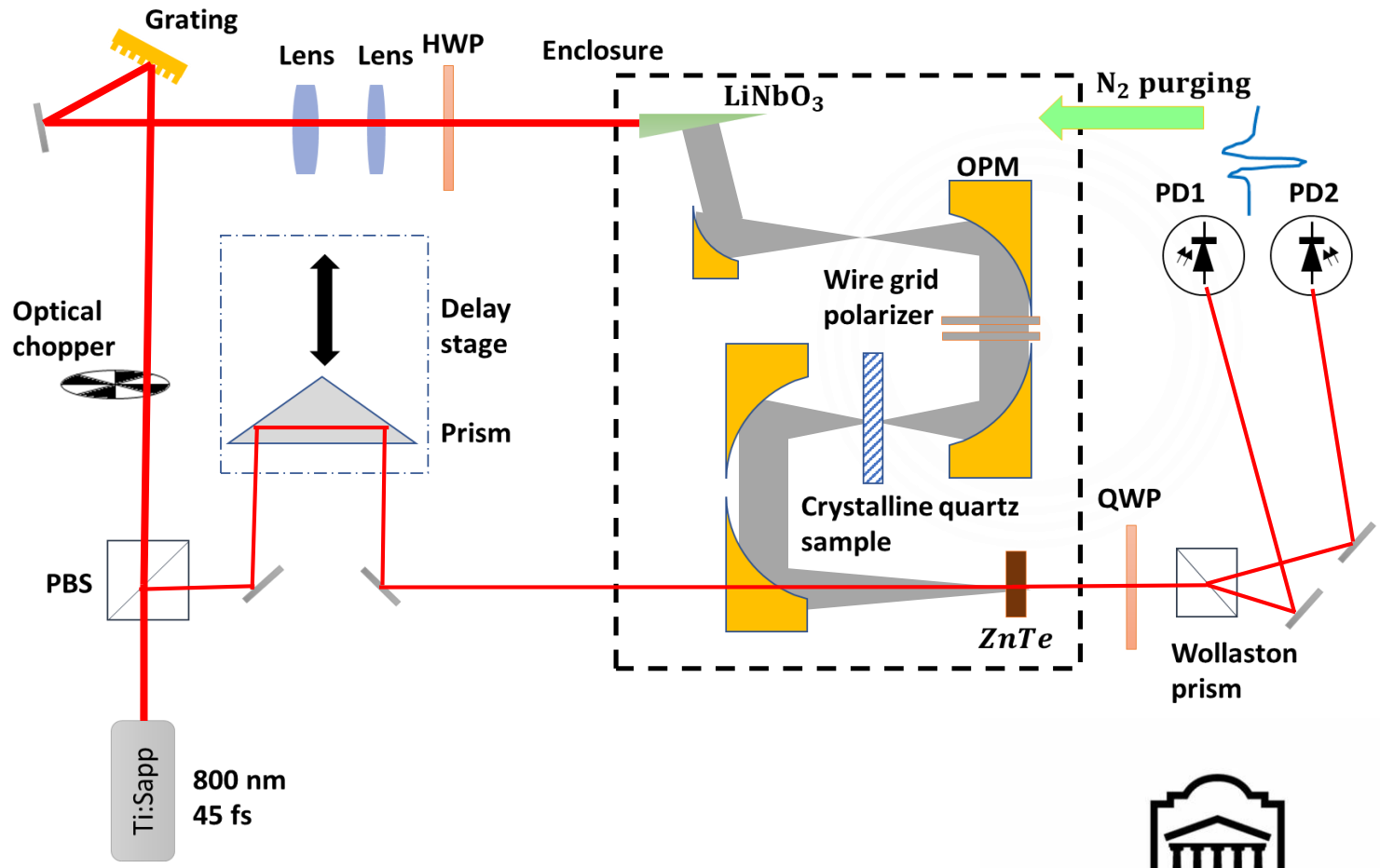

Nonlinear Delay

- Intense field → modified

refractive index: $n = n_0 + n_2 I$

- $\Delta\phi = \underbrace{n_0\, k_0 L}_{\text{Linear phase}} + \underbrace{n_2 I\, k_0\, L}_{\text{Nonlinear phase}}$

- $f(t-\tau) \overset{F}{\leftrightarrow} F(\omega)e^{-i\tau\omega}$

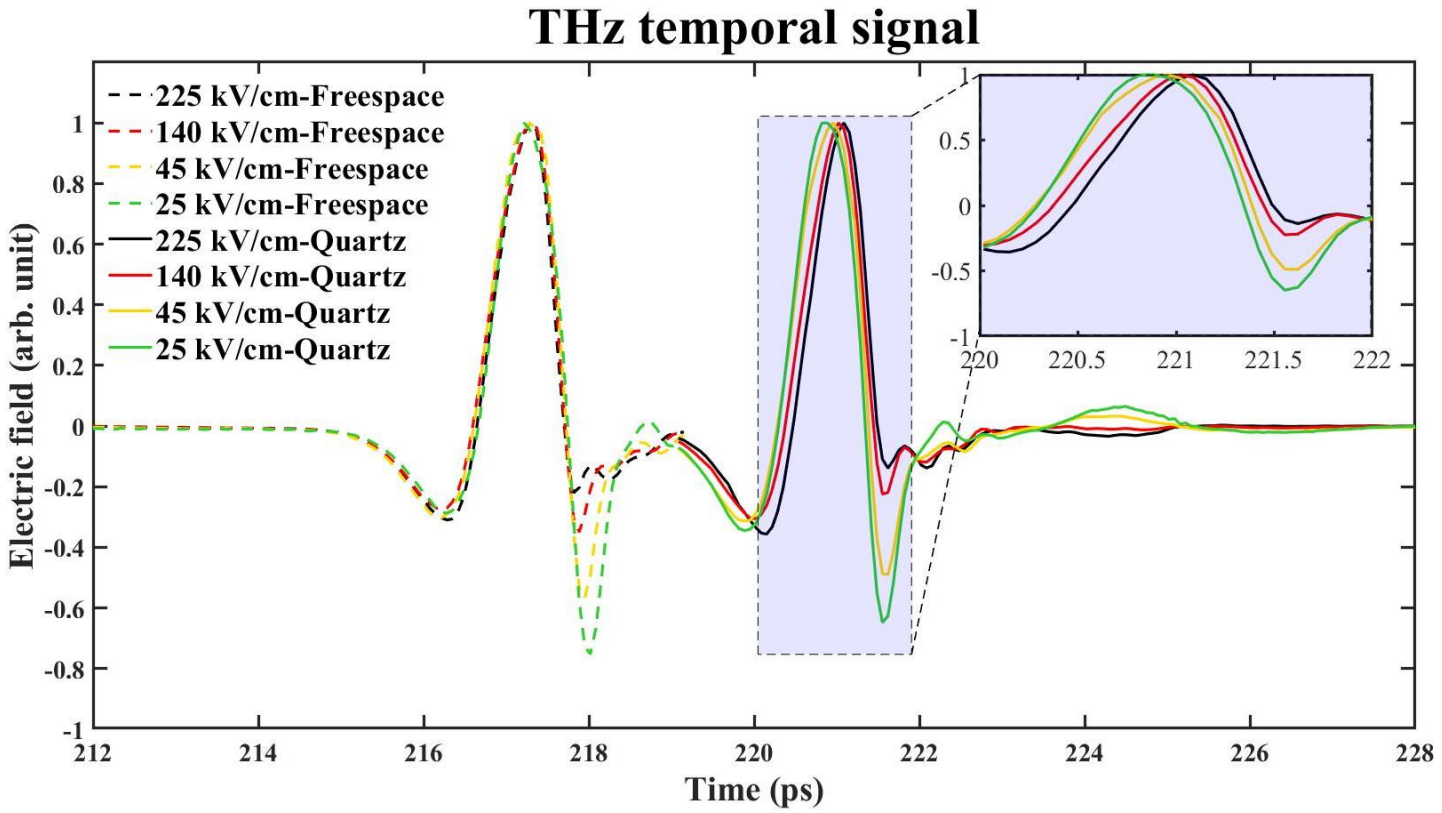

Higher intensity → more delay

Average Time Shift

- Main lobe
- Lowest signal level (25 kV/cm)

  as linear response
- Average time delay

$$t_{\mathrm{av}}^{i} = \mathrm{avg}\left(\sum_{k} t(V_i = V_k) - t(V_{\mathrm{low}} = V_k)\right)$$

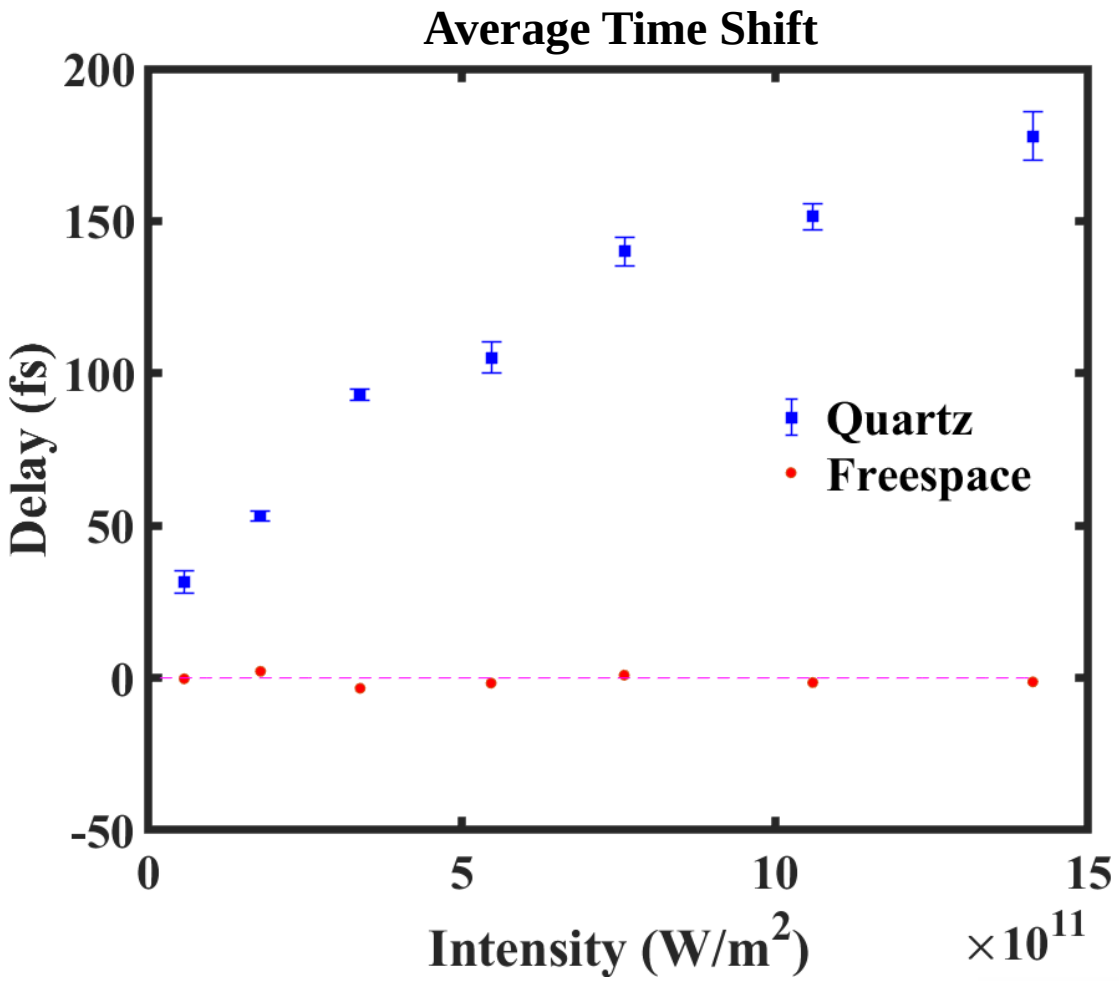

Fourier Domain

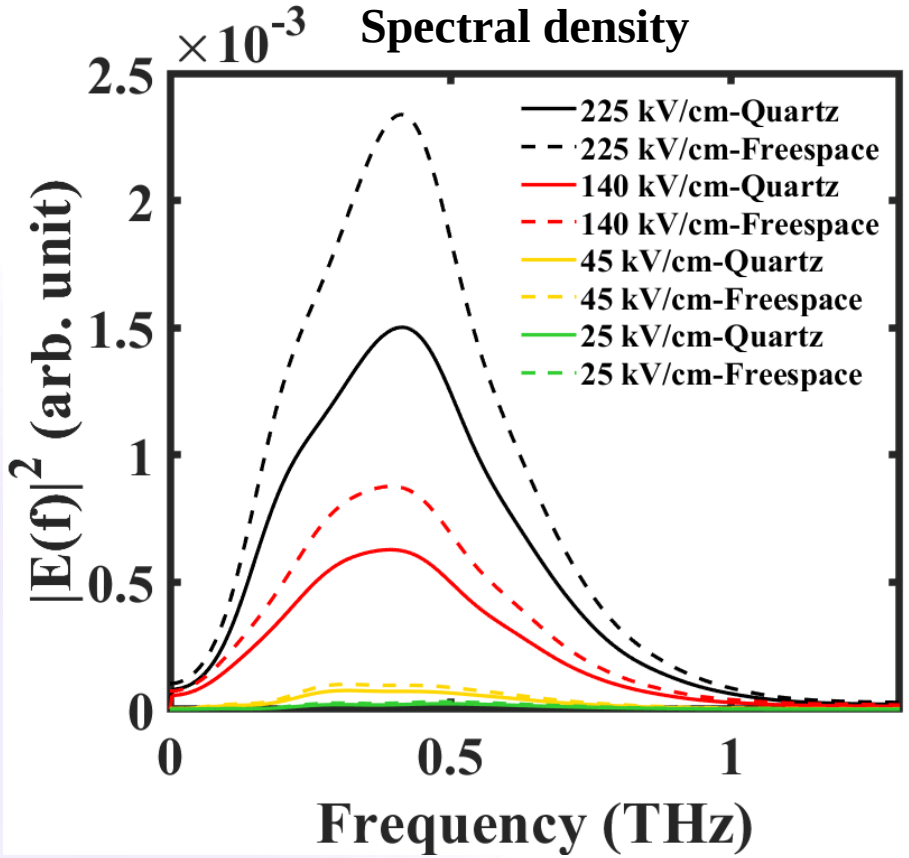

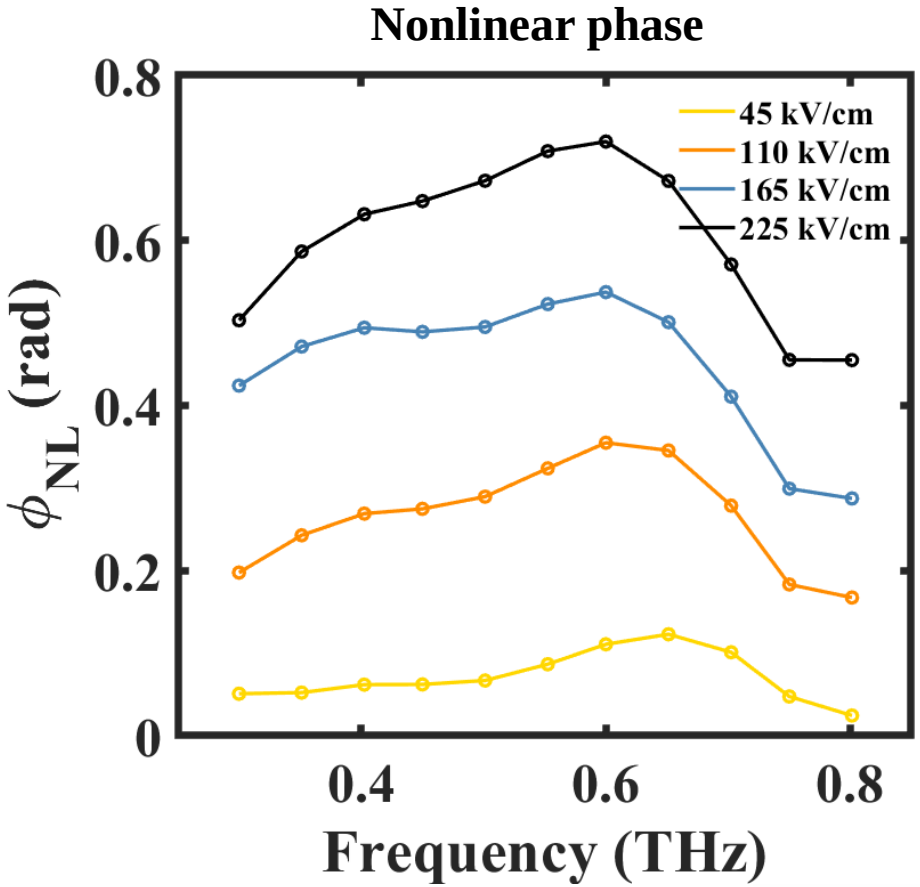

Absorption Spectrum

- Difference between Freespace (dashed) and quartz sample (solid)

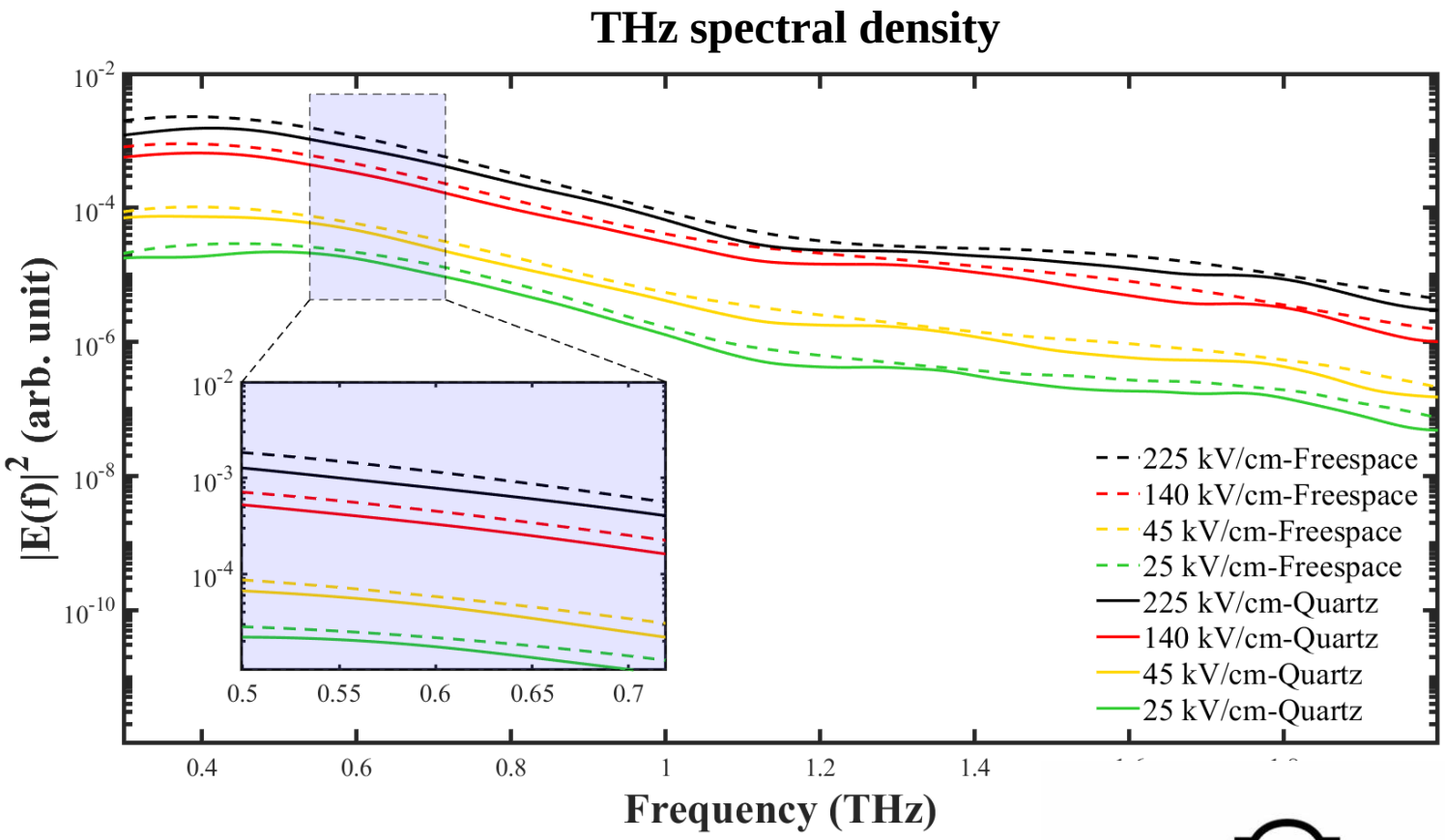

Nonlinear Response

- n_2 → several orders of magnitude larger than optical value
- Negative real part $\chi^{(5)}$
- Monochromatic field vs wideband pulse

Measured nonlinear phase @ 0.4 THz

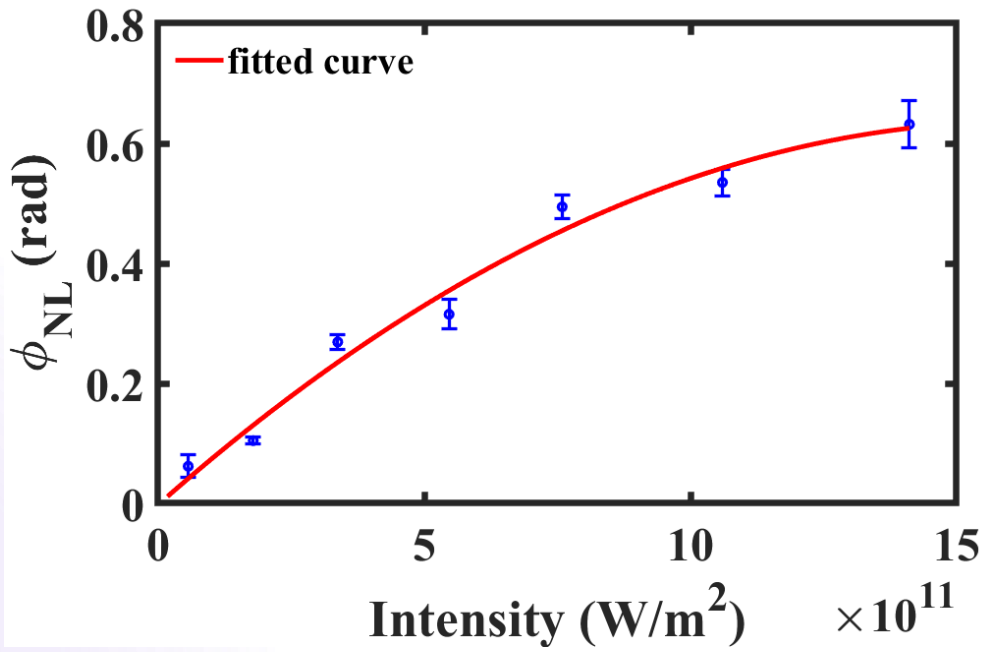

Measured absorption coefficient @ 0.4 THz

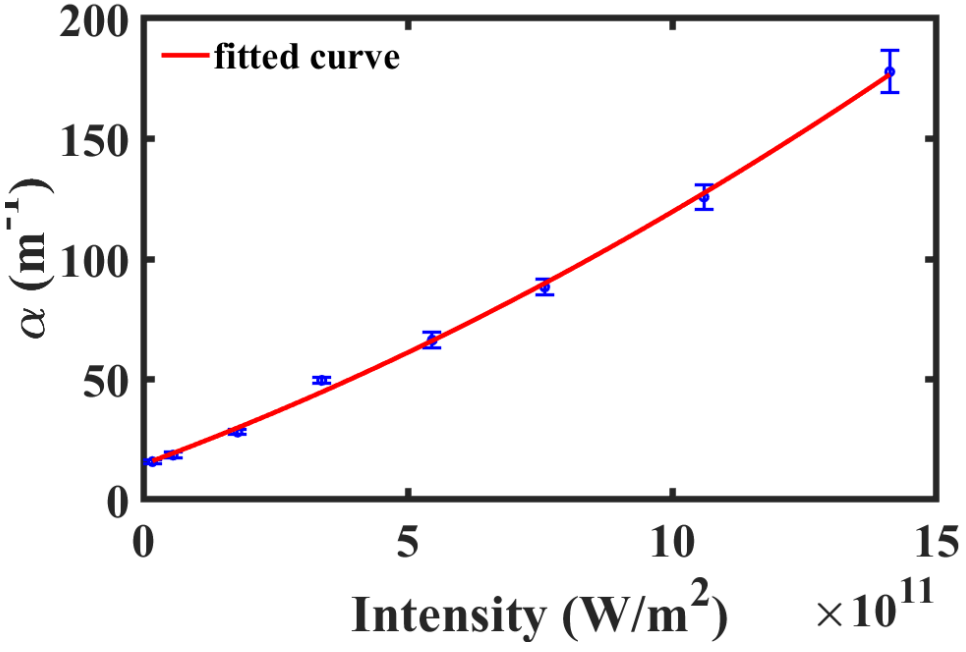

$$\chi^{(3)} = 1.40 \times 10^{-15} + i7.49 \times 10^{-17}\ \mathrm{m^2/V^2}$$
$$\rightarrow n_2 = 9.00 \times 10^{-14}\ \mathrm{m^2/W}$$

$$\chi^{(5)} = -2.68 \times 10^{-30} + i1.49 \times 10^{-31}\ \mathrm{m^4/V^4}$$

Suppression of Self-Focusing for Few-Cycle Pulses

In all cases, $P = 4\ P_{cr}$

N = Number of cycles in input pulse

Propagation direction is downward.

GVD suppresses self-focusing

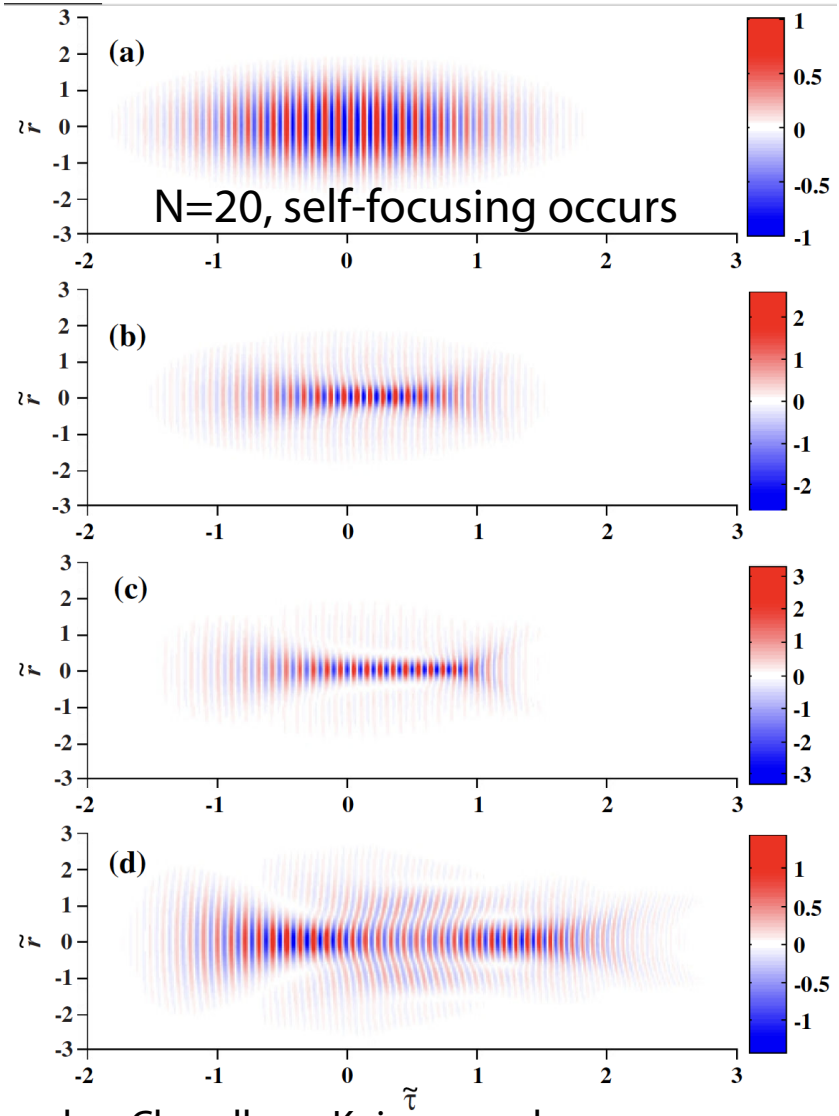

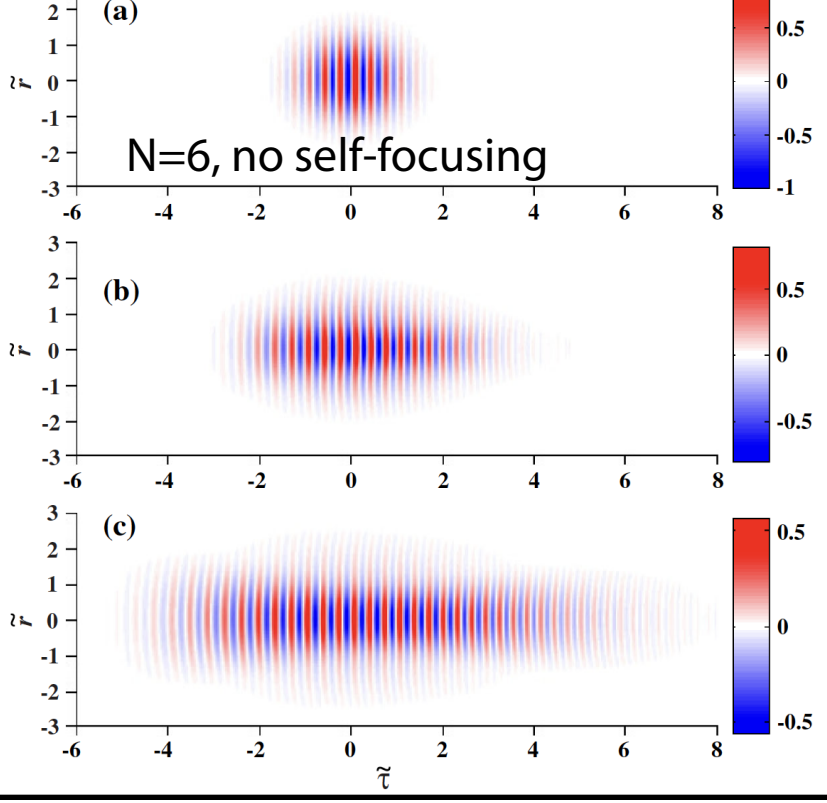

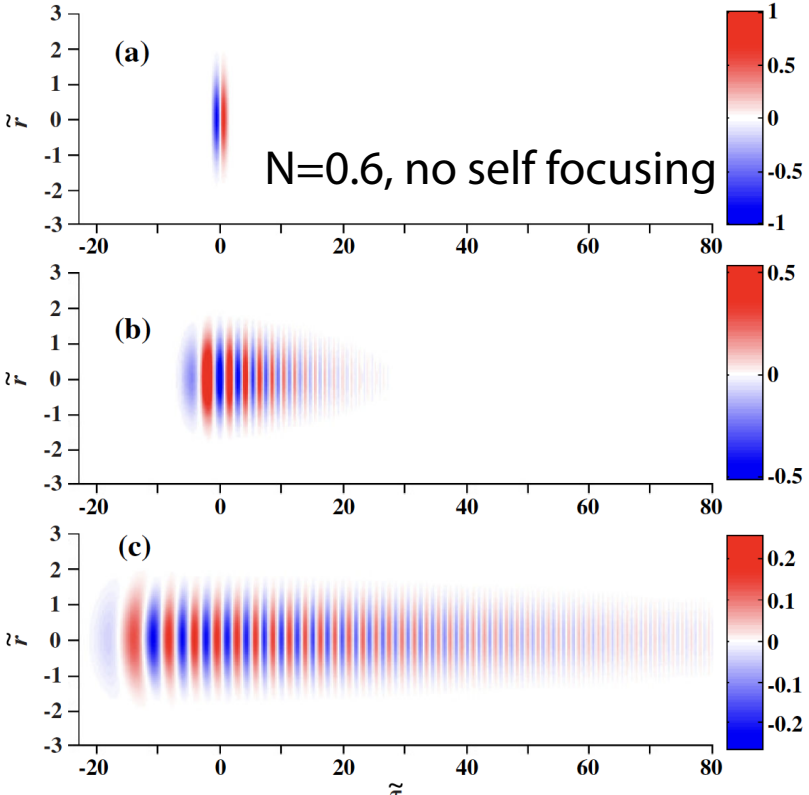

Kozlov, Drozdov, Choudhary, Kniazev, and Boyd, J. Opt. Soc. Am. B 36,G68 (2019).

Broadband THz Bandpass Spectral Filters Based on Multilayer Metasurfaces

Joint project with Iridian Spectral Technologies
Project led by Ali Makeki and Jean-Michel Ménard

- Dielectric metasurfaces
- Plasmonic metasurfaces
  - Easy to fabricate (unlike dielectric structures)
  - low plasmonic loss (unlike visible-NIR region)

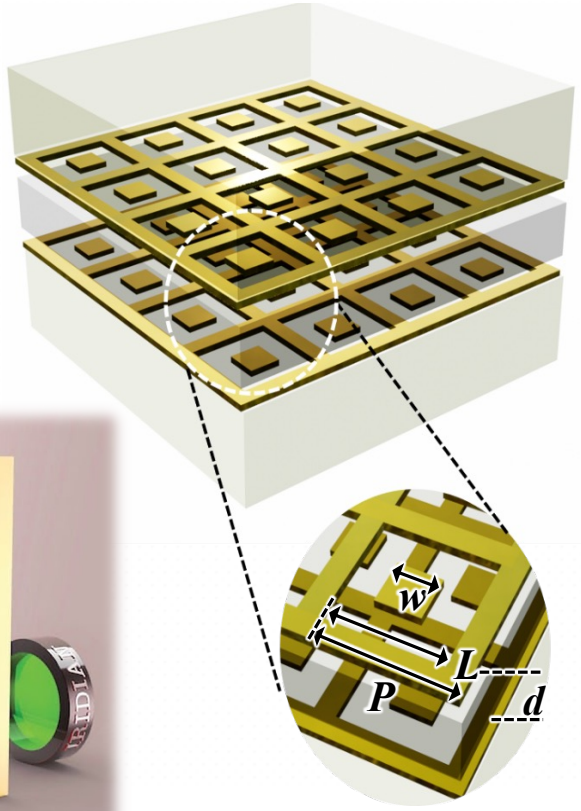

Transmission can be controlled by flooding the filter with visible light.

Gingras et al., Optics Express 28, 395508 (2020)
Maleki et al., Photonics Research 11, 526 (2023)

Some Comparisons

1. FIR and THz

Light-matter interaction largely due to phonons, vibrational degree of freedom
Strong light-matter coupling, leading for example to restrahlen bands

2. Visible Light and Soft UV

Light-matter interaction largely due to response of bound electrons
Light-matter coupling is weaker than for vibrational degree of freedom

3. Short Ultraviolet

Light-matter interaction largely due to free electrons
Strong light-matter coupling, leading to the plasmonics

Light-matter interactions can lead to a negative dielectric permittivity for 1 and 3, but not for 2.

Acknowledgments

This work was supported by the Natural Sciences and Engineering Research Council of Canada, the Canada Research Chairs program, the U.S. Office of Naval Research, and the U.S. National Science Foundation.

I thank all of my students and postdocs in the US and Canada.

Rochester Group

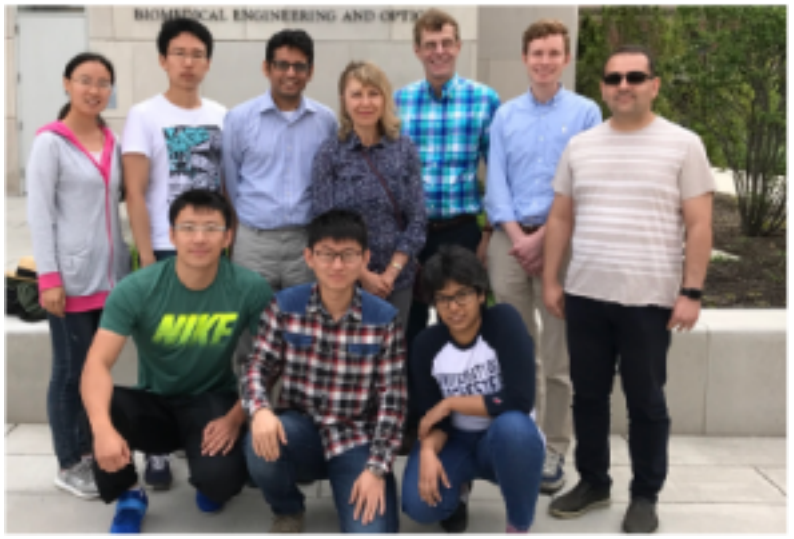

Ottawa Group